International Journal of Engineering

Journal Homepage: www.ije.ir

Fingertip Radius Effect of an on-Surface-Manipulated Object

S. Hadian Jazi*[a], P. Rasouli[b], M. Keshmiri[b]

[a] *Department of Mechanical Engineering, University of Isfahan, Isfahan, Iran.*
[b] *Department of Mechanical Engineering, Isfahan University of Technology, Isfahan, Iran.*

PAPER INFO

Paper history:
Received 21 August 2016
Received in revised form 09 October 2016
Accepted 05 January 2017

Keywords:
Slip/Roll Contact
Slippage Control
Grasping
Multi-Robot Systems
Dynamic Modeling

ABSTRACT

Cooperative arms are two or more arms in series which assume the structure of a parallel robot on account of gripping an intermediary object, and are commonly used in accurate assembly industries, coaxialization, movement of object, etc. Gripping an intermediary object is one of the complicated subjects in analysis of cooperative arms, whose analysis is mostly dependent upon the manner the object is gripped by the arms fingertips. In the case of griping objects in frictional manner, the elimination of unwanted slippage of fingertips on the object due to the environmental factors, and also the effect of the fingertips geometry on the movement equations are among the major topics in such arms analysis. The dynamic analysis and control synthesis of the undesired slippage between an object and robot fingertips in object manipulation and the effects of finger radius or geometry of the fingertip on the function dynamics and slippage control is studied in this article. The slip/roll contact model is applied in the dynamic formulation and analysis of the finger geometry the effects of which are studied using numerical simulation.

doi: *10.5829/idosi.ije.2017.30.01a.17*

1. INTRODUCTION

In object manipulation, the contact between fingertips and an object is a challenging issue drawing the attention of researchers in the field. The contact type and condition, finger geometry and softness, grasping force conditions, stability as well as maneuverability are some of the issues encountered in recent decades.

Reuleaux was the first to introduce the force and form closure concept [1]. Many researchers have used the closure concept to analyze object grasping in order to find the conditions for a closure grasp. A number of researchers have presented algorithms which help find the appropriate contact points on the object for closure grasp. What is common to all of these studies is the assumption that there is no slippage between the fingertips and the object [2-7].

Since slippage is possible during object manipulation, its presence in the dynamic modeling would result in a more complete model. Cole et al., [8], Kao and Cutkosky, [9],and Xin Zhi et. al. [10], were among the first to consider the slippage to improve the grasping skills in robots manipulating objects. In their studies, slippage was a predefined process where the path and time of the fingertips slippage on the object were completely determined. In other words, they applied slippage for the purpose of re-grasping to improve the maneuverability of robot manipulation.

Motamedi et al. used a haptic device and vision based sensors to detect slippage in a grasped object [11]. Dzitac et al. presented new approaches to find minimum amount of sensors required for preventing slip in a grasping [12]. They found that in a two-sensor combination using the normal grasp force and the tangential force, sensors has the best performance.

Cordella et al. used an experimental system to detect normal forces for slip detection purposes and then presented a control strategy for slip preventing in a prosthetic hand [13].

The authors of this article have extended the issue with respect to a dynamic analysis and control of undesired slippage during object manipulation in their previous studies. Introducing a new model for frictional contact, they developed an algorithm to control any undesired slippage during object manipulation [14-16].

*Corresponding Author's Email: *s.hadian@eng.ui.ac.ir* (S. Hadian Jazi)

Please cite this article as: S. Hadian Jazi, P. Rasouli, M. Keshmiri, Fingertip Radius Effect of an on-Surface-Manipulated Object, International Journal of Engineering (IJE), TRANSACTIONS A: Basics Vol. 30, No. 1, (January 2017) 134-142

In these studies the robot fingertip is assumed to be very sharp; hence, its geometry is disregarded, making the authors turn to the slip/stick contact model in the analysis. The studies conducted and the control algorithms proposed were assessed by both numerical simulation and experimental analysis. The results obtained indicate the proper capability of the controller needed to control undesired slippages.

Although these studies have improved the dynamical modeling, it is still a long way from the impractical and hypothetical assumption of geometry-free fingertip-and-sharp contact.

To further improve the dynamic modeling, the fingertips geometry is used for modeling the same in this article where the effect of fingertip geometry on undesired slippage control is analyzed. This study was conducted by manipulating an object on a surface using a single manipulator to contribute to undesired slippage control. Here, the slip/stick model was replaced with the slip/rolling model.

2. SYSTEM EQUATIONS OF MOTION

A schematic of the system is presented in Figure 1. The system consists of a double-link manipulator equipped with a spherical fingertip. There is no constraint on the slippage of the fingertip at the contact point. The whole motion of the system is assumed to be planar. The contact between the object and the fingertip is still a point contact with the potential of both slipping and rolling for the fingertip on the object surface.

For this system, the following assumptions are in order:

1. At the contact points only a normal and tangential forces are applied. No moment is applied to the surfaces.
2. The object is constantly in contact with the surface and has no rotation.
3. The friction coefficients at the upper and lower surfaces of the object are represented by μ_1 and μ_2 respectively. Obviously, the condition $\mu_1 > \mu_2$ is necessary for the object to move.

In order to present the equations of motion for the system, the model is divided into four subsystems: manipulator, object, contact model or frictional constraints and kinematic constraints.

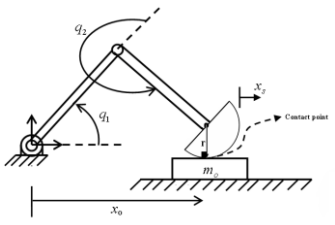

Figure 1. A schematic of the target system

The following is a description of each subsystem together with their respective equations.

2. 1. Manipulator Equations of Motion Considering the forces on the fingertip (Figure 2), equations of motion for the manipulator is given by:

$$\mathbf{M}\ddot{\mathbf{q}} + \mathbf{h} = \boldsymbol{\tau} - \mathbf{J}^T \mathbf{F}_1 \tag{1}$$

where $\mathbf{F}_1$ is the force applied to the fingertip from the object's upper surface; $\mathbf{M}$, a 2×2 manipulator inertia matrix, $\mathbf{h}$, a 2×1 vector, contributing to gravitation, centrifugal and Coriolis forces; $\mathbf{J}$, a 2×2 Jacobian matrix; $\boldsymbol{\tau}$, a 2×1 applied torque vector; and $\mathbf{q} = [q_1 \quad q_2]^T$ the arm's joints position vector shown in Figure 1. The details of the matrices are presented in Appendix A.

2. 2. Object Equations of Motion An object-free body diagram is shown in Figure 3. Equations of motion for this subsystem in the x and y directions are as follows:

$$\mathbf{M}_o \ddot{x}_o + \mathbf{h}_o = \mathbf{W}\mathbf{F} \tag{2}$$

where x_o is the object displacement in the x direction with respect to the inertial reference frame (see Figure 1), $\mathbf{M}_o$, $\mathbf{h}_o$, $\mathbf{F}$ and $\mathbf{W}$ are defined as follows:

$$\mathbf{M}_o = \begin{bmatrix} m_o \\ 0 \end{bmatrix}, \ \mathbf{h}_o = \begin{bmatrix} 0 \\ m_o g \end{bmatrix}, \quad \mathbf{F} = \begin{bmatrix} \mathbf{F}_1 \\ \mathbf{F}_2 \end{bmatrix}, \ \mathbf{W} = \begin{bmatrix} 1 & 0 & 1 & 0 \\ 0 & 1 & 0 & 1 \end{bmatrix}. \tag{3}$$

where m_o is the object mass, g gravity acceleration, $\mathbf{F}_2$ force applied from the surface to the object. As shown in Figure 3, forces $\mathbf{F}_1$ and $\mathbf{F}_2$ are projected on a normal-tangential coordinate attached to the object.

2. 3. Kinematic Constraint Equations The fingertip connection to the object surface must not be disturbed as it would otherwise lead to the following geometric constraints.

$$\mathbf{A}_q \ddot{\mathbf{q}} + \mathbf{A}_o \ddot{x}_o + \mathbf{A}_s \ddot{x}_s = \mathbf{b} \tag{4}$$

where

$$\mathbf{A}_q = \mathbf{J}, \ \mathbf{A}_o = \mathbf{A}_s = \begin{bmatrix} -1 \\ 0 \end{bmatrix}, \ \mathbf{b} = -\dot{\mathbf{A}}_q \dot{\mathbf{q}} - \dot{\mathbf{A}}_o \dot{x}_o - \dot{\mathbf{A}}_s \dot{x}_s \tag{5}$$

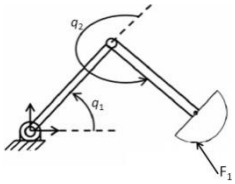

Figure 2. A schematic of the one-finger manipulator and the force exerted on its fingertip

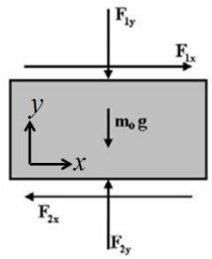

Figure 3. Object free-body diagram

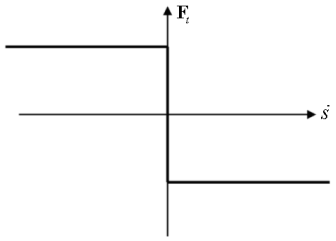

Figure 5. Change of the friction force with respect to slippage speed

x_S is the amount of fingertip slippage on the object, measured from the initial contact point.

2. 4. Frictional Contact Equations In our previous studies, a new model was developed for slip-stick friction contact conditions [14]. In this study, a similar model is to be developed for slip-roll friction contact. Figure 4 shows the fingertip in contact with the object surface.

The value s is the slippage displacement of the fingertip on the object surface measured in the tangential direction. Clearly, the slippage velocity vector with a speed of $\dot{s}$ is tangential to the surface. In this Figure, F_t and F_n are tangential and normal forces exerted on the fingertip from the surface of the object at the contact point.

To model the friction contact conditions, the following assumptions are in order:

1. The fingertip contacts the object contact at a single point;
2. The fingertip either slips or rolls on the object;
3. The static and dynamic friction coefficients are similar; and
4. The positive normal direction of the tangential-normal coordinate attached to the object points towards the center of the object curvature

This last assumption is to guarantee that the positive normal force enforces the fingertip-object connection. Negative normal force means separation of the fingertip from the object, a phenomenon was not assumed in this study.

According to the above assumptions, a change of friction force with respect to slippage speed is presented in Figure 5.

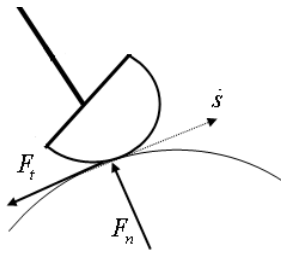

Figure 4. The fingertip-object contact

Accordingly, the following conditions for the contact between the fingertip and the object can be realized at any point in time:

1. The fingertip slips on the object: $\dot{s} \neq 0$;
2. The relative velocity of the fingertip with respect to the object is zero: $\dot{s} = 0$ in case one of the following condition occurs:
   a. The fingertip continues rolling on the object: $\ddot{s} = 0$;
   b. The fingertip stops rolling and starts slipping: $\ddot{s} > 0$ or $\ddot{s} < 0$;
   c. The fingertip stops slipping and starts rolling: $\ddot{s}^{-} \neq 0$ and $\ddot{s} = 0$; and
   d. The fingertip is slipping but changes the slippage direction: $\ddot{s}^{-}\ddot{s} < 0$

All of the above conditions are tabulated in Table 1.

In this table, $\ddot{s}^{-}$ is the slippage acceleration at $t - dt$.
The equations in Table 1 can be expressed in a combined form as a single equation as follows:

$$\alpha_1 \ddot{s} + \mathbf{DF} = 0 \tag{6}$$

where

$$\mathbf{D} = \begin{bmatrix} \alpha_2 & \alpha_3 \mu \end{bmatrix}, \mathbf{F} = \begin{bmatrix} F_t & F_n \end{bmatrix}^T \tag{7}$$

And $\alpha_1, \alpha_2, \alpha_3$ are switching coefficients selected from Table 2.

TABLE 1. Different kinematic conditions of contact

Kinematic conditions			Equation
Slippage ($\dot{s} \neq 0$)			$F_t = -\mu F_n \text{sign}(\dot{s})$
Zero relative velocity ($\dot{s} = 0$)	Continuous rolling ($\ddot{s}^{-} = 0$ and $\ddot{s} = 0$)		$\ddot{s} = 0$
	Slippage start ($\ddot{s}^{-} = 0$)	Forward ($\ddot{s} > 0$)	$F_t = -\mu F_n$
		Backward ($\ddot{s} < 0$)	$F_t = \mu F_n$
	Slippage stop ($\ddot{s}^{-} \neq 0$ and $\ddot{s} = 0$)		$\ddot{s} = 0$
	Reversing ($\ddot{s}^{-} \neq 0$ and $\ddot{s} \neq 0$)		$F_t = 0$

TABLE 2. Switching coefficients in Equation (6)

	$\dot{s}\neq 0$	$\dot{s}=0$				
		$\ddot{\bar{s}}\neq 0$			$\ddot{\bar{s}}=0$	
	Slippage	Slippage Reversing	Slippage stop	Continuous Rolling	Slippage start (Forward)	Slippage start (Backward)
α_1	0	0	1	1	0	0
α_2	1	1	0	0	1	1
α_3	$\text{sign}(\dot{s})$	0	0	0	1	1

The main advantage of Equation (6) is its representation in a second-order ordinary differential equation form which can easily be associated with the other dynamics equation.

Therefore, for the upper surface, the contact conditions can be described by

$$\beta_1\ddot{x}_s+\mathbf{D}_1\mathbf{F}_1=0 \tag{8}$$

while, for the lower surface of the object, the condition is described as:

$$\alpha_1\ddot{x}_o+\mathbf{D}_2\mathbf{F}_2=0 \tag{9}$$

where

$$\mathbf{D}_1=\begin{bmatrix}\beta_2 & \beta_3\mu_1\end{bmatrix},\ \mathbf{D}_2=\begin{bmatrix}\alpha_2 & \alpha_3\mu_2\end{bmatrix} \tag{10}$$

and μ_1 and μ_2 are the friction coefficients at the upper and lower surfaces, respectively.

The package of the governing equations for this system is presented below. It should be noted that the last two equations are the ones introduced above.

$$\begin{aligned}&\mathbf{M}\ddot{\mathbf{q}}+\mathbf{h}=\boldsymbol{\tau}-\mathbf{J}^T\mathbf{F}_1,\ \mathbf{M}_o\ddot{x}_o+\mathbf{h}_o=\mathbf{WF}\\&\mathbf{A}_q\ddot{\mathbf{q}}+\mathbf{A}_o\ddot{x}_o+\mathbf{A}_s\ddot{x}_s=\mathbf{b}\\&\beta_1\ddot{x}_s+\mathbf{D}_1\mathbf{F}_1=0,\ \alpha_1\ddot{x}_o+\mathbf{D}_2\mathbf{F}_2=0\end{aligned} \tag{11}$$

It should be noted that, in a stick/slip contact model, a similar equation and the related table can be used; if so, the rolling condition is replaced by the stick condition.

3. CONTROL SYNTHESIS

In order to control the system, the above package, (11), with a proper definition of inputs and outputs is initially converted to an input-output descriptive form. The actuating torque vector $\boldsymbol{\tau}=\begin{bmatrix}\tau_1 & \tau_2\end{bmatrix}^T$ and the state vector $\mathbf{x}=\begin{bmatrix}x_o & x_s\end{bmatrix}^T$ are selected as the input and output 2×1 vectors, respectively.

In order to materialize the input-output descriptive form, the $\mathbf{F}_1$, $\mathbf{F}_2$ and $\ddot{\mathbf{q}}$ are eliminated from the package of the governing Equations (11) and in the meantime, with a few simple matrix operations, the following equation is obtained:

$$\tilde{\mathbf{M}}\ddot{\mathbf{x}}+\tilde{\mathbf{h}}=\tilde{\mathbf{B}}\boldsymbol{\tau} \tag{12}$$

where $\tilde{\mathbf{M}}$, a 2×2 matrix, $\tilde{\mathbf{h}}$, a 2×1 vector, and $\tilde{\mathbf{B}}$, a 2×2 matrix, are defined as:

$$\begin{aligned}&\tilde{\mathbf{M}}=\begin{bmatrix}\mathbf{D}_1\mathbf{M}_J\mathbf{A}_x & \beta_1+\mathbf{D}_1\mathbf{M}_J\mathbf{A}_x\\ \alpha_1+\mathbf{D}_2(\mathbf{M}_o-\mathbf{M}_J\mathbf{A}_x) & -\mathbf{D}_2\mathbf{M}_J\mathbf{A}_x\end{bmatrix},\\&\mathbf{M}_J=\mathbf{J}^{-T}\mathbf{M}\mathbf{J}^{-1},\ \tilde{\mathbf{h}}=\begin{bmatrix}-\mathbf{D}_1\left(\mathbf{M}_J\mathbf{b}+\mathbf{J}^{-T}\mathbf{h}\right)\\ \mathbf{D}_2\left(\mathbf{M}_J\mathbf{b}+\mathbf{J}^{-T}\mathbf{h}+\mathbf{h}_o\right)\end{bmatrix},\\&\mathbf{b}=-\dot{\mathbf{J}}\dot{\mathbf{q}},\qquad \tilde{\mathbf{B}}=\begin{bmatrix}-\mathbf{D}_1\\ \mathbf{D}_2\end{bmatrix}\mathbf{J}^{-T}\end{aligned} \tag{13}$$

The outstanding characteristic of the equation presented in (12) is that it is written in the conventional form of equations for the motion of robotic systems. Matrix $\tilde{\mathbf{M}}$ in this equation is invertible and the equation is internally stable. The proof of these two properties is presented in [14].

Equation (12) represents a multi-phase system with the following phases:

1. The object is moving on the selected surface and the fingertip is slipping on the upper surface of the object;
2. The object is moving on the selected surface and the fingertip is rolling on the upper surface of the object;
3. The object is at rest on the selected surface and the fingertip is slipping on the upper surface of the object; and
4. The object is at rest on the selected surface and the fingertip is rolling on the upper surface of the object.

In phase 1, the system has two degrees of freedom. The controller must be able to reduce the tracking errors of the object and control the fingertip slippage on the object.

In phase 2, since there is no slippage between the fingertip and the object, the controller must only reduce the tracking errors of the object and since there are two actuating inputs, these tracking errors control can be satisfied along with the input torque optimization. The optimization must not influence the non-slippage condition of the fingertip.

In phases 3 and 4 where the object is at rest on the select surface, the controller should be able to return the object in the motion mode. Put otherwise, it should move back to the 1st or 2nd phase.

This observation indicates that the system controller must also be a multiphase controller presented as follows:

Phase 1: Matrix $\tilde{\mathbf{B}}$ is reversible and a conventional CTM controller is proposed as follows:

$$\boldsymbol{\tau} = \tilde{\mathbf{B}}^{-1}\left(\tilde{\mathbf{M}}\left(\ddot{\mathbf{x}}^{des} + \mathbf{K}_v\dot{\mathbf{e}} + \mathbf{K}_p\mathbf{e}\right) + \tilde{\mathbf{h}}\right), \quad (14)$$

where $\mathbf{K}_p$ and $\mathbf{K}_v$ are positive definite constant matrices and

$$\mathbf{x}^{des} = \begin{bmatrix} x_o^{des} & x_s^{des} \end{bmatrix}^T. \quad (15)$$

where x_o^{des} represent the desired trajectory of the object. For x_s^{des} it should be noted that here the desired value for x_s is assumed to be zero. This means that the controller seeks to stop the fingertip slippage and return the fingertip to the initial contact point; hence,

$$\mathbf{e} = \begin{bmatrix} e_o \\ e_s \end{bmatrix} = \begin{bmatrix} x_o^{des} - x_o \\ 0 - x_s \end{bmatrix}. \quad (16)$$

Inserting (14) in (12), the error dynamics is written as:

$$\ddot{\mathbf{e}} + \mathbf{K}_v\dot{\mathbf{e}} + \mathbf{K}_p\mathbf{e} = \mathbf{0}, \quad (17)$$

which indicates that in this phase, the controller presented in (14) forces the error to converge to zero. Hence, it can be deduced that during this phase, while the controller reduces the object tracking error, it seeks to stop the fingertip slippage and put the system into phase 2. In fact, the controller increases the normal force on the upper surface in order to increase the friction forces on both surfaces of the object and uses these friction forces as the controlling forces.

Phase 2: The $\tilde{\mathbf{B}}$ matrix is not invertible and the proposed controller is presented as follows:

$$\boldsymbol{\tau} = \tilde{\mathbf{B}}^{\#}\left(\tilde{\mathbf{M}}\left(\ddot{\mathbf{x}}^{des} + \mathbf{K}_v\dot{\mathbf{e}} + \mathbf{K}_p\mathbf{e}\right) + \tilde{\mathbf{h}}\right) + \left(\mathbf{I}_{2\times 2} - \tilde{\mathbf{B}}^{\#}\tilde{\mathbf{B}}\right)\mathbf{y}, \quad (1)$$

where $\mathbf{y}_{2\times 1}$ is an arbitrary vector and $\tilde{\mathbf{B}}^{\#}$ is Moore–Penrose pseudoinverse of $\tilde{\mathbf{B}}$. The matrices $\mathbf{K}_p$, $\mathbf{K}_v$ and the vectors $\mathbf{x}^{des}$ and $\mathbf{e}$ are defined as before except that $\mathbf{K}_p$ is a positive semi-definite constant matrix.

As mentioned earlier, in this phase, the implied forces on the object can be somehow optimized, i.e. $\mathbf{y}$ can be selected in a manner where, in addition to keeping the rolling mode at the upper surface unchanged, the implied forces are optimized. For this purpose, the norm of the internal forces is selected as the optimization cost function; therefore, the optimization algorithm is expressed by:

$$\text{Minimize} \quad \left\| \begin{bmatrix} \mathbf{F}_1 \\ \mathbf{F}_2 \end{bmatrix} \right\|$$

Such that

$$\boldsymbol{\tau} = \tilde{\mathbf{B}}^{\#}\left(\tilde{\mathbf{M}}\left(\ddot{\mathbf{x}}^{des} + \mathbf{K}_v\dot{\mathbf{e}} + \mathbf{K}_p\mathbf{e}\right) + \tilde{\mathbf{h}}\right) + \left(\mathbf{I}_2 - \tilde{\mathbf{B}}^{\#}\tilde{\mathbf{B}}\right)\mathbf{y} \quad (19)$$

$$\mathbf{J}^T\mathbf{F}_1 = -\left(\mathbf{M}\ddot{\mathbf{q}} + \mathbf{h}\right) + \boldsymbol{\tau}\ ,\ \mathbf{F}_1 + \mathbf{F}_2 = \mathbf{M}_o\ddot{x}_o + \mathbf{h}_o\ ,$$

$$\mathbf{J}\ddot{\mathbf{q}} = \mathbf{b}\ ,\ \tilde{\mathbf{M}}\ddot{\mathbf{x}} + \tilde{\mathbf{h}} = \tilde{\mathbf{B}}\boldsymbol{\tau}\ ,\ \left[1 \quad \sigma\mu_1 sign\left(\dot{x}_o^{des}\right)\right]\mathbf{F}_1 = 0$$

Selecting $0 < \sigma < 1$, guarantees that the friction force at the upper surface of the object stays in the friction cone. By inserting (1) in (12) and forming the error equation, the error convergence to zero can be observed.

Phase 3: In this phase, the fingertip is in slippage mode and the object is at rest; hence, $\mathbf{D}_2 = \mathbf{0}$. The controller should make the object move and put the system in either phase 1 or 2. This controller is defined the same as in phase 2 with the difference that $\mathbf{D}_2$ is replaced by $\mathbf{D}_2^{ref}$.

$$\mathbf{D}_2^{ref} = \left[1 \quad \mu_2 sign\left(\dot{x}_o^{des}\right)\right], \quad (20)$$

Similar to phase 1, the controller increases the friction forces through an increase in the normal forces and makes the object move in a limited time span since the friction coefficient on the upper surface is greater than that on the lower surface.

Phase 4: In this phase, both $\mathbf{D}_1$ and $\mathbf{D}_2$ matrices are zero. In order to move the object, the controller is defined the same as in phase 1 with the difference that $\mathbf{D}_1$ and $\mathbf{D}_2$ are replaced by $\mathbf{D}_1^{ref}$ and $\mathbf{D}_2^{ref}$, respectively.

$$\mathbf{D}_1^{ref} = \left[1 \quad \mu_1 sign\left(\dot{x}_o^{des}\right)\right], \mathbf{D}_2^{ref} = \left[1 \quad \mu_2 sign\left(\dot{x}_o^{des}\right)\right] \quad (21)$$

Like phase 1, the controller increases the friction forces through an increase in the normal forces and makes the object move in a limited time span since the friction coefficient on the upper surface is greater than that on the lower surface.

Parameters m_1 and m_2 are the mass of the first and second links; and l_1 and l_2 are the lengths of the first and second links. Parameters $\bar{\mu}_1$ and $\bar{\mu}_2$ are the nominal values of the friction coefficients for the upper and lower surfaces, respectively. The nominal values are applied to the controller to determine the actuating torques.

4. NUMERICAL RESULTS

The numerical values of the system parameters for the numerical simulation purposes are presented in TABLE 3.

The assumption is that the links are uniform. A rectilinear motion path with the following trapezoidal speed profile is considered as the desired path for the object:

$$\ddot{x}_o^{des} = \begin{cases} 0.0256 & 0 < t < 1 \\ 0 & 1 \le t < 6 \\ -0.0256 & 6 \le t < 7 \end{cases}, \quad \begin{matrix} \dot{x}_o^{des}(0) = 0 \\ x_o^{des}(0) = 1.366 \end{matrix} \quad (22)$$

In order to simulate an undesired slippage, it is assumed that the real value of μ_1 is the same as the nominal value and the real value of μ_2 different from

the nominal value as follows:

$$\mu_2 = \begin{cases} 0.15 & 0.5 < t < 4 \\ \bar{\mu}_2 & \text{elsewhere} \end{cases} \quad (23)$$

This means that the lower surface friction coefficient in a portion of the path differs from that of the rest. For the fingertip, $r = 0,10,17\ (cm)$ is used in the simulation. The zero value represents the sharp contact and stick-slip model.

The simulation results are presented in Figures 6-16. The position of the contact point on the upper surface of the object is illustrated in Figure 6. The object position error with respect to the desired path is illustrated in Figure 7. The object speed change is shown in Figure 8. The speed and value of the fingertip slippage on the upper surface of the object are shown in Figures 9 and 10, respectively. As observed in Figures 9 and 10, no slippage occurs on the upper surface prior to the t=0.5 second (when μ_2 differs from $\bar{\mu}_2$ and the motion is disturbed). During this period, the object tracks its desired path down with almost no errors (Figures 7 and 8). Afterwards, the fingertip begins to slip on the upper surface and the object diverts from its desired path, and eventually stops. As observed in Figure 8, it takes about 0.5 seconds for the controller to make the object move again. Once the object begins to move again, the controller seeks to eliminate the fingertip slippage while making the object track the desired trajectory (Figure 8). The fingertip slippage is finally controlled in about 0.7 seconds. This pattern is true for all the three fingertip radii.

The tangential and normal forces on both surfaces of the object are shown in Figures 11 - 14. These diagrams indicate the fact that once the disturbance and slippage begin, the controller eliminates the slippage by increasing the normal force and promotes the object motion while compensating for the trajectory tracking error.

The actuation moment of the first and the second acuator is shown in Figures 15 and 16, respectively.

Figure 6 illustrates that when the fingertip radius is zero and there is no slippage, the contact point remains fixed while when the radius is different from zero, the slip-roll contact condition, the contact point comes back slowly towards its initial position on the upper surface even after elimination of slippage.

TABLE 3. Values of the system parameters

$l_1(m)$	$l_2\ (m)$	$m_1\ (kg)$	$m_2\ (kg)$	$m_o\ (kg)$	$\bar{\mu}_1$	$\bar{\mu}_2$
1	1	1	1	2.5	0.25	0.1

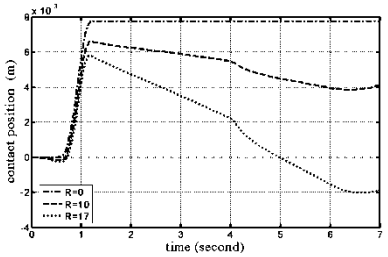

Figure 6. Time history of contact point position on the object in meter

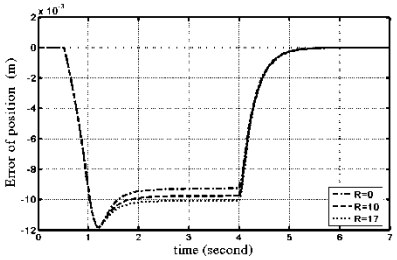

Figure 7. Time history of the object position error in meter

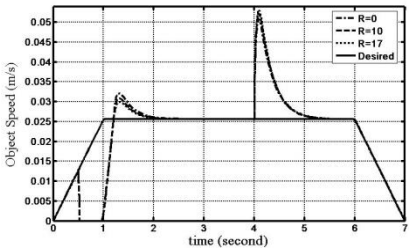

Figure 8. Time history of Object speed in meter per second

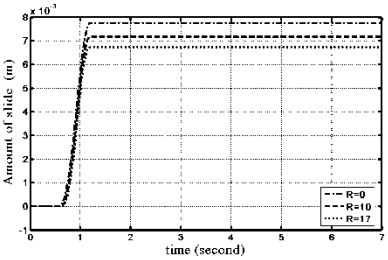

Figure 9. Time history of fingertip slippage on the object in meter

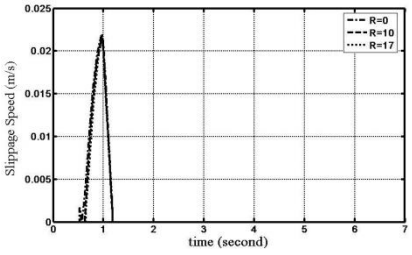

Figure 10. Time history of fingertip slippage speed on the object in meter per second

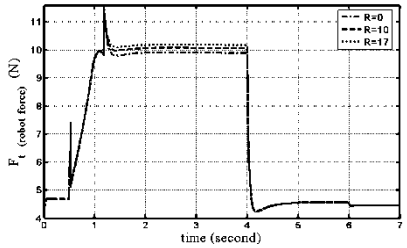

Figure 11. Time history of tangential forces exerted on the upper surface of the object in Newton

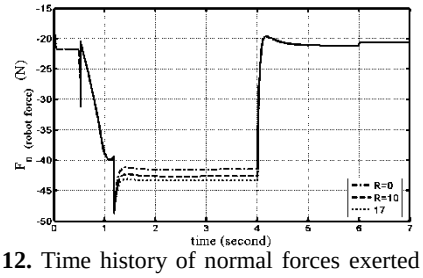

Figure 12. Time history of normal forces exerted on the upper surface of the object in Newton

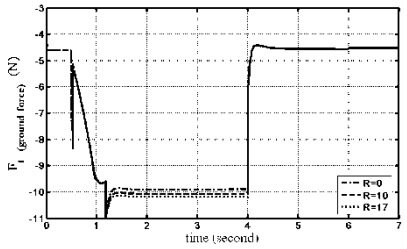

Figure 13. Time history of tangential forces exerted on the lower surface of the object in Newton

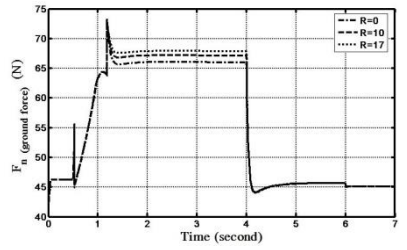

Figure 14. Time history of normal forces exerted on the lower surface of the object in Newton

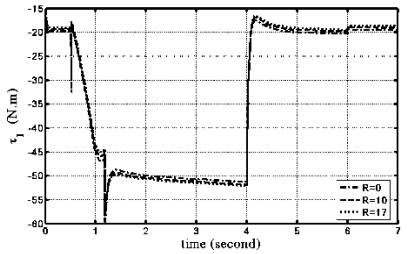

Figure 15. Time history of the moment of first acuator in N.m

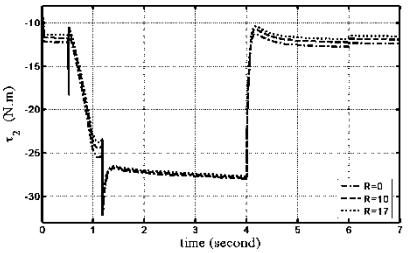

Figure 16. Time history of the moment of second acuator in N.m

5. CONCLUSION

This article has extended the previous studies on the undesired slippage control of the manipulator fingertips manipulating an object by considering the fingertip radius and slip-roll contact condition. Using slip-roll contact between manipulator end-effector and the grasped object and investigating the effect of the shape of the end-effector on the control of undesired slippage in grasping is the main innovation of this paper. In the previous works, authors assumed point contact between end-effecor and the grasped object. For this purpose, the previous dynamic model and control strategies are modified. This study has focused on the effect of the fingertip radius on the system's dynamics and controller performance. The numerical simulations of the proposed multi-phase controller indicated that the controller is capable of eliminating the fingertip slippage within a limited time span. In this study, if r=0, the results can be exactly like those of the previous study. In addition, it is inferred that a bigger fingertip radius contributes to a slightly better performance.

6. APPENDIX A

The contributing vectors and matrices in Equation (1) for the target manipulator are as follows:

$$\mathbf{M}=\begin{bmatrix} M_{11} & M_{12} \\ M_{21} & M_{22} \end{bmatrix}$$
$$M_{11}=\bar{I}_1+\bar{I}_2+m_2l_1^2+2m_2l_1l_{c2}\cos(q_2)$$
$$M_{12}=M_{21}=\bar{I}_2+m_2l_1^2+m_2l_1l_{c2}\cos(q_2) \quad (A.1)$$
$$M_{22}=\bar{I}_2$$
$$\bar{I}_1=m_1l_{c1}^2+I_1\ ,\ \bar{I}_2=m_2l_{c2}^2+I_2$$

$$\mathbf{h}=\begin{bmatrix} h_1 \\ h_2 \end{bmatrix}$$
$$h_1=-m_2l_1l_{c2}(2\dot{q}_1+\dot{q}_2)\dot{q}_2\sin(q_2) \quad (A.2)$$
$$+\ (m_1l_{c1}+m_2l_1)g\cos(q_1)+m_2gl_{c2}\cos(q_1+q_2)$$
$$h_2=m_2gl_{c2}\cos(q_1+q_2)+m_2l_1l_{c2}\dot{q}_1^2\sin(q_2)$$

$$\mathbf{J}=\begin{bmatrix} J_{11} & J_{12} \\ J_{21} & J_{22} \end{bmatrix}$$
$$J_{11}=-l_1\sin(q_1)-l_2\sin(q_1+q_2)+r$$
$$J_{12}=-l_2\sin(q_1+q_2)+r \qquad (A.3)$$
$$J_{21}=l_1\cos(q_1)+l_2\cos(q_1+q_2)$$
$$J_{22}=l_2\cos(q_1+q_2)$$

where $m_k, l_k, (l_c)_k, I_k, k=1,2$ represent the mass, length, position of the center of the mass, and inertia moment of the kth link of the manipulator, respectively and r the fingertip radius.

7. REFERENCES

1. Reuleaux, F., "The kinematics of machinery: Outlines of a theory of machines, Dover, (1963).
2. Salisbury, J.K. and Roth, B., "Kinematic and force analysis of articulated mechanical hands", ***Journal of Mechanisms, Transmissions and Automation in Design-Transactions of the Asme***, Vol. 105, No. 1, (1983), 35-41.
3. Platt, R., Fagg, A.H. and Grupen, R.A., "Nullspace composition of control laws for grasping", in Intelligent Robots and Systems, IEEE/RSJ International Conference on, Lausanne, Switzerland. Vol. 2, (2002), 1717-1723
4. XiangYang, Z. and Han, D., "Computation of force-closure grasps: An iterative algorithm", ***Robotics, IEEE Transactions on***, Vol. 22, No. 1, (2006), 172-179.
5. Zheng, Y. and Qian, W.H., "An enhanced ray-shooting approach to force-closure problems", ***Journal of Manufacturing Science and Engineering-Transactions of the ASME***, Vol. 128, No. 4, (2006), 960-968.
6. Shapiro, A., Rimon, E. and Shoval, S., "On the passive force closure set of planar grasps and fixtures", ***The International Journal of Robotics Research***, Vol. 29, No. 11, (2010).
7. Rosales, C., Ros, L., Porta, J.M. and Suárez, R., "Synthesizing grasp configurations with specified contact regions", ***The International Journal of Robotics Research***, Vol. 30, No. 4, (2011), 431-443.
8. Cole, A.A., Ping, H. and Sastry, S.S., "Dynamic control of sliding by robot hands for regrasping", ***Robotics and Automation, IEEE Transactions on***, Vol. 8, No. 1, (1992), 42-52.
9. Kao, I. and Cutkosky, M.R., "Comparison of theoretical and experimental force/ motion trajectories for dextrous manipulation with sliding", ***The International Journal of Robotics Research***, Vol. 12, No. 6, (1993), 529-534.
10. Xin Zhi, Z., Nakashima, R. and Yoshikawa, T., "On dynamic control of finger sliding and object motion in manipulation with multifingered hands", ***Robotics and Automation, IEEE Transactions on***, Vol. 16, No. 5, (2000), 469-481.
11. Motamedi, M.R., Chossat, J.B., Roberge, J.P. and Duchaine, V., "Haptic feedback for improved robotic arm control during simple grasp, slippage, and contact detection tasks", IEEE International Conference on Robotics and Automation (ICRA), Stockholm, Sweden. (2016), 4894-4900.
12. Dzitac, P., Mazid, A.M., Ibrahim, M.Y., Appuhamillage, G.K. and Choudhury, T.A., "Optimal sensing requirement for slippage prevention in robotic grasping", International Conference on Industrial Technology (ICIT), Seville, Spain. (2015), 373-378.
13. Cordella, F., Gentile, C., Zollo, L., Barone, R., Sacchetti, R., Davalli, A., Siciliano, B. and Guglielmelli, E., "A force-and-slippage control strategy for a poliarticulated prosthetic hand", in IEEE International Conference on Robotics and Automation (ICRA), Stockholm, Sweden. (2016), 3524-3529.
14. Hadian Jazi, S., Keshmiri, M. and Sheikholeslam, F., "Dynamic analysis and control synthesis of grasping and slippage of an object manipulated by a robot", ***Advanced Robotics***, Vol. 22, No. 13-14, (2008), 1559-1584.
15. Hadian Jazi, S., Keshmiri, M., Sheikholeslam, F., Ghobadi Shahreza, M. and Keshmiri, M., "Dynamic analysis and control synthesis of undesired slippage of end-effectors in a cooperative grasping", ***Advanced Robotics***, Vol. 26, (2012), 1693–1726.
16. Hadian Jazi, S., Keshmiri, M., Sheikholeslam, F., Ghobadi Shahreza, M. and Keshmiri, M., "Adaptive manipulation and slippage control of an object in a multi-robot cooperative system", ***Robotica***, Vol. 32, No. 05, (2014), 783-802.

Fingertip Radius Effect of an on-Surface-Manipulated Object

S. Hadian Jazi[a], P. Rasouli[b], M. Keshmiri[b]

[a] *Department of Mechanical Engineering, University of Isfahan, Isfahan, Iran.*
[b] *Department of Mechanical Engineering, Isfahan University of Technology, Isfahan, Iran.*

P A P E R I N F O

Paper history:
Received 21 August 2016
Received in revised form 09 October 2016
Accepted 05 January 2017

Keywords:
Slip/Roll Contact
Slippage Control
Grasping
Multi-Robot Systems
Dynamic Modeling

چکیده

سیستم‌های رباتیکی همکار از دو یا چند بازوی رباتیکی تشکیل شده‌اند که به‌منظور انجام عملیات خاصی روی اجسام مورد استفاده قرار می‌گیرند. این نوع از سیستم‌ها که ساختاری مشابه با ربات‌های موازی دارند کاربردهای متفاوتی مانند مونتاژ دقیق قطعات، جابجایی اجسام و غیره دارند. تحلیل گرفتن جسم توسط سیستم‌های همکار یکی از مهم‌ترین، و در عین حال پیچیده‌ترین تحلیل‌ها در این سیستم‌هاست. یکی از روش‌هایی که برای گرفتن اجسام در این‌گونه سیستم‌ها استفاده می‌شود، گرفتن اصطکاکی است، یعنی همان روشی که در سیستم‌های طبیعی مانند دست انسان استفاده می‌شود. در این حالت است که امکان وقوع لغزش‌های ناخواسته بین پنجه ربات و جسم وجود دارد و حذف یا کنترل این لغزش‌ها می‌تواند موضوع بسیار مهمی در تحلیل رفتار این سیستم‌ها باشد. به‌همین دلیل در این مقاله اثر شکل سرپنجه ربات در دینامیک و کنترل لغزش‌های ناخواسته بین سرپنجه ربات و جسمی که توسط ربات گرفته‌شده مورد بررسی قرار گرفته است. برای این منظور نوع تماس لغزشی-غلتشی و پنجه ربات در حالت دو بعدی به شکل نیم دایره در نظر گرفته شده و اثر شعاع پنجه روی حرکت جسم، لغزش و کنترل آن بررسی شده است.

***doi**: 10.5829/idosi.ije.2017.30.01a.17*